Adaptive Dead-Time Control in a Resonant Wireless Power Transfer System

Tim Krigar, Martin Pfost
TU Dortmund University
Martin-Schmeisser-Weg 4
44227 Dortmund, Germany
Phone: +49 231-7556731
Email: tim.krigar@tu-dortmund.de
URL: https://ewa.etit.tu-dortmund.de/

Acknowledgments

This work was supported by the German Federal Ministry of Education and Research under grant 16ES1023. The authors are responsible for the content of this publication.

Keywords

≪Wireless power transmission≫, ≪Contactless Power Supply≫, ≪Parasitics≫, ≪Zero-voltage switching≫, ≪Dead-time≫

Abstract

The influence of parasitic capacitances and of the output load on the ZVS behavior of a resonant wireless power transfer system is analyzed in this work. For this, the charging process of the output capacitors of a GaN-based inverting half bridge is described in detail. Furthermore, the influence of the parasitic capacitances and of the load on the resonant current is discussed.

The analyzed system has a peak efficiency of 92.9 % at 500 W with an operating frequency of 2 MHz. Based on the ZVS analysis, an adaptive dead-time control is presented to raise the average efficiency. For example, the efficiency can be raised by 0.5 % while transferring 250 W.

Introduction

To avoid bulky cables or abrasive brushes, wireless power transfer (WPT) systems are attractive for modern industrial applications to supply moving actuators. The most common WPT systems are inductive WPT (iWPT) systems with capacitors to compensate the large stray inductances of the weakly coupled transmitting and receiving coil. (Other approaches exist that use capacitive WPT, but iWPT has the advantage that the transmission ratio can be changed by the turn number ratio.)

In compact iWPT systems, high switching frequencies in the MHz range are needed, which asks for soft switching capability of the half bridge stage of the primary side. To realize zero voltage switching (ZVS), a resonant LLC topology can be used as shown in [1, 2]. In MHz range resonant converter systems, the dead-time has to be set particularly accurate to achieve ZVS and high efficiency. The ZVS capability is heavily influenced by the load, by the switching frequency, and by parasitic capacitances, see [3–6].

This paper presents an analysis of the ZVS capability of a 2 MHz 500 W resonant WPT system with step-down characteristic from 400 V to 48 V. Based on this analysis, an adaptive dead-time control of the WPT system without any communication with the receiving side is presented. This control scheme improves the efficiency over a wide range and is very attractive for WPT systems with a passive receiving side.

System Overview

Fig. 1 shows an overview of the proposed system. The rectangular voltage v_{sw} is generated by a half bridge consisting of two GaN HEMTs (GS66508T), the operating frequency is 2 MHz. The use of GaN HEMTs enables fast switching due to their small parasitic capacitances and because they do not exhibit a reverse-recovery effect. Especially in resonant systems with ZVS and operating frequencies in the MHz range, the output capacitances of the half bridge switches must be small to enable a fast charging and discharging process of the switching node.

The half bridge supplies the resonant network formed by the resonant capacitor C_r, the transmitting coil L_1, and the center-taped receiving coil L_{2a}/L_{2b}, cf. Fig. 1. The system uses an LLC topology to compensate the stray inductances. For this, the all-primary-referred equivalent circuit of the transformer is used, see Fig. 2. The stray inductances are aggregated in L_r. L_m is the mutual inductance of the transformer. This topology achieves a compensation with only one capacitor on the primary side of the iWPT system. The input voltage of 400 V is stepped down to an output voltage of 48 V. With only two rectifying diodes, the receiving side is kept passive and simple.

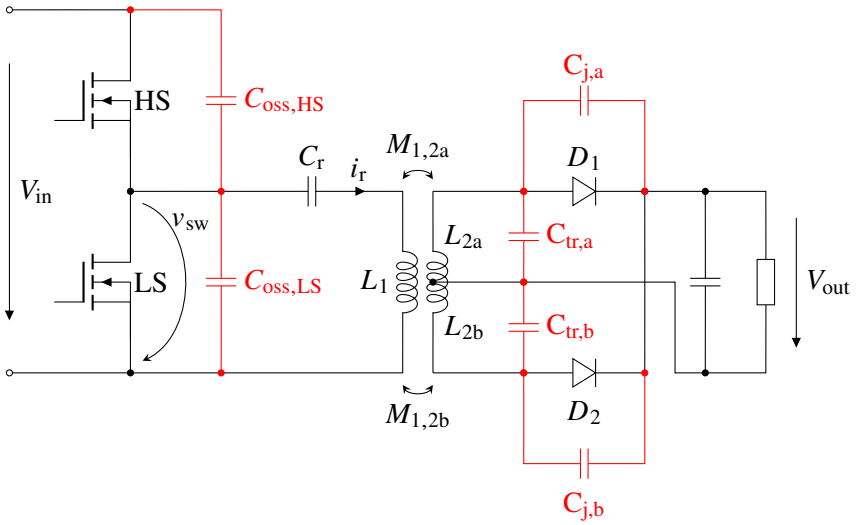

Fig. 1: Schematic of components are shown in black with the parasitic capacitances in red.

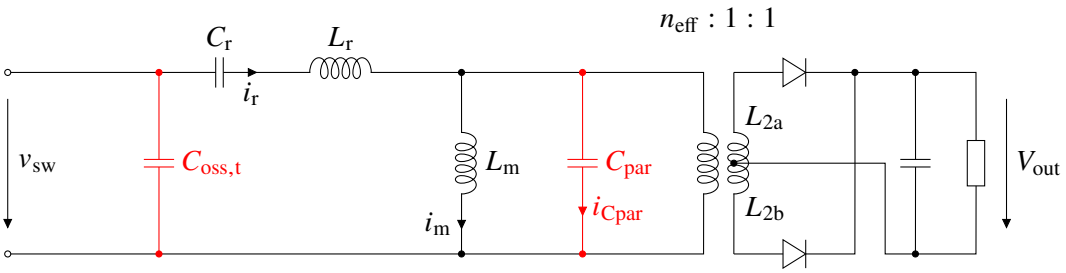

Fig. 2: All-primary-referred equivalent circuit. The parasitic capacitances which influence the ZVS behavior are marked red.

$C_{oss,HS}$ and $C_{oss,LS}$ are the effective output capacitances of the GaN HEMTs. They are summarized in the total output capacitance in Fig. 2 as

$$C_{oss,t} = C_{oss,HS} + C_{oss,LS}. \tag{1}$$

The junction capacitors of the rectifying diodes are represented by $C_{j,a}$ and $C_{j,b}$. $C_{tr,a}$ and $C_{tr,b}$ are the parasitic capacitances of the receiving coils L_{2a} and L_{2b}. Note that parasitic capacitances between the receiving and the transmitting coil can be neglected due to the large air gap of 5 mm between the coils

of the WPT system. For circuit analysis, the receiving side parasitic capacitances are summarized and transferred to the primary side in Fig. 2 as

$$C_{\mathrm{par}} = \frac{1}{n_{\mathrm{eff}}^2}(C_{\mathrm{j,a}} + C_{\mathrm{tr,a}} + C_{\mathrm{j,b}} + C_{\mathrm{tr,b}}). \tag{2}$$

Dead-Time Analysis

During the dead-time, $C_{\mathrm{oss,t}}$ is charged by the resonant current $i_{\mathrm{r}}(t)$, cf. Figs. 1 and 2, to provide ZVS capability. This process is influenced by several factors, especially by C_{par} and by the output power P_{out}. To analyze this behavior of the iWPT system, circuit simulation is used. The values of the components and of the parasitic capacitances which are used in the simulation are listed in Tab. I. The results of the simulation can be seen in Fig. 3.

Note that only a switch-on event is shown, because a switch-off event behaves the same way, only negated. The figure includes three columns, where the first column is a reference column. It shows the behavior of the analyzed system with a summarized parasitic capacitance $C_{\mathrm{par}} = 50\,\mathrm{pF}$ while transferring 500 W. The other two columns show the system behavior with varying C_{par} (middle column) and P_{out} (right column).

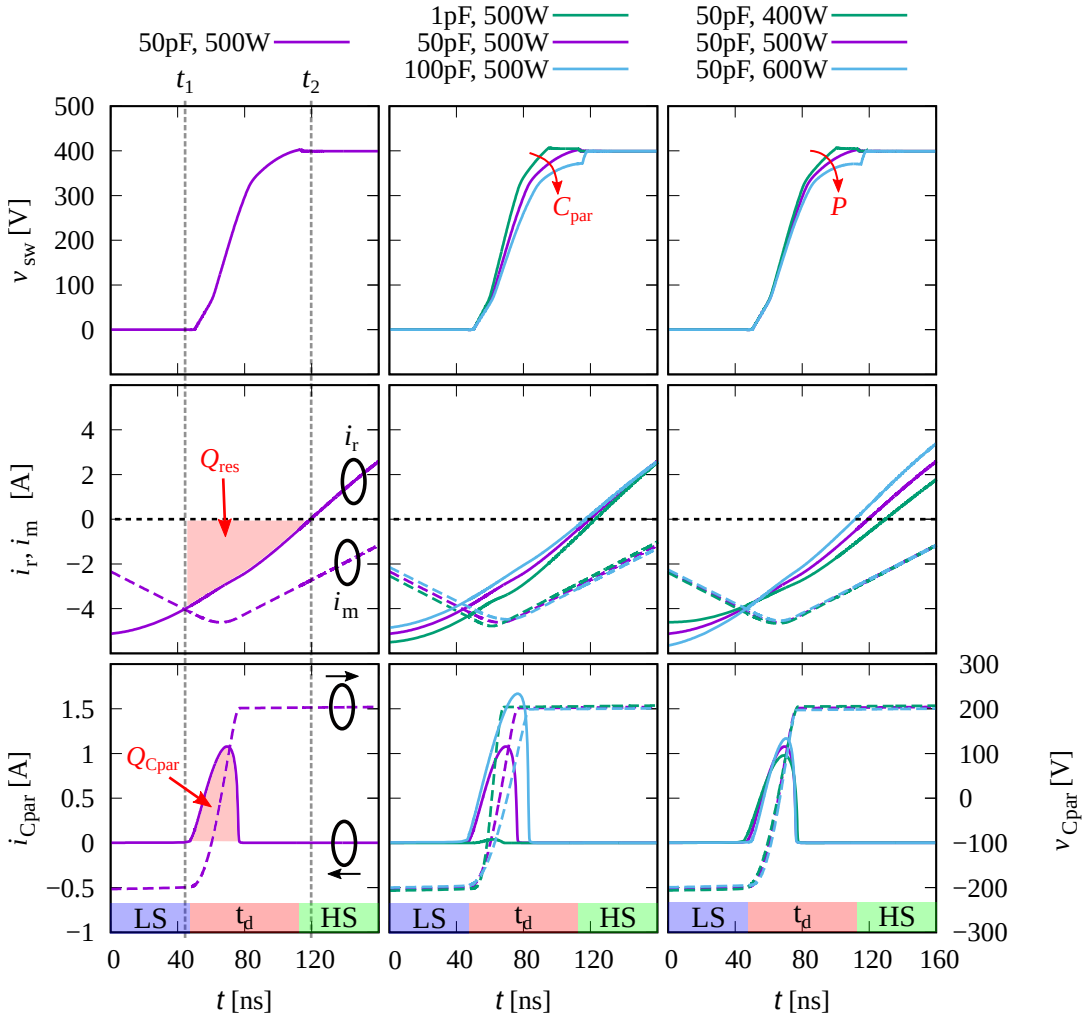

Fig. 3: ZVS behavior dependencies of the presented system with $t_{\mathrm{d}} = 65\,\mathrm{ns}$. Left column: proposed system with $C_{\mathrm{par}} = 50\,\mathrm{pF}$ and $P_{\mathrm{out}} = 500\,\mathrm{W}$. Center column: influence of the parasitic capacitance C_{par} from 1 pF to 100 pF. Right column: influence of output power for P_{out} from 400 W to 600 W.

Table I: Simulation parameters

C_r	690 pF
L_r	8.8 μH
L_m	5.26 μH
$C_\mathrm{oss,t}$	200 pF
C_par	50 pF
n_eff	4.11
V_in	400 V

There are two time points t_1 and t_2 that have to be considered. At t_1, the resonant and magnetizing current intersect (middle row in Fig. 3). The resonant current $i_\mathrm{r}(t)$ then starts to charge the parasitic capacitances, which results in an increase in voltage V_m across the mutual inductance of the transformer (bottom row in Fig. 3). The required charge must be considered in addition to the charge which is needed to charge $C_\mathrm{oss,t}$ to 400 V, which is why the parasitic capacitances influence the ZVS behavior of the system. The charging process of $C_\mathrm{oss,t}$ begins together with the dead-time. At t_2, the resonant current crosses zero. After that, $i_\mathrm{r}(t)$ discharges $C_\mathrm{oss,t}$. Thus, the dead-time should not exceed t_2. The maximum available charge Q_res of the resonant current can be calculated as

$$Q_\mathrm{res} = \int_{t_1}^{t_2} i_\mathrm{r}(t)\,\mathrm{d}t. \tag{3}$$

$i_\mathrm{r}(t)$ is determined using the fundamental harmonic approximation as described in [7]:

$$i_\mathrm{r}(t) = \frac{v_\mathrm{1,sw}(t)}{Z_\mathrm{eq}} = \frac{v_\mathrm{1,sw}(t)}{i\omega L_\mathrm{r} + \dfrac{1}{i\omega L_\mathrm{m} - \dfrac{i}{\omega L_\mathrm{m}} + \dfrac{1}{R_\mathrm{ac}}} - \dfrac{i}{\omega C_\mathrm{r}}} \quad \text{with} \quad R_\mathrm{ac} = {n_\mathrm{eff}}^2 \frac{8}{\pi^2} R_\mathrm{L}. \tag{4}$$

This complex expression contains α, the phase shift between $v_\mathrm{1,sw}(t)$ and $i_\mathrm{r}(t)$, and $|i_\mathrm{r}(t)|$. Both are defined as

$$\alpha = \angle i_\mathrm{r}(t) = \operatorname{atan}\left[R_\mathrm{ac}\left(\left(\omega C_\mathrm{par} - \frac{1}{\omega L_\mathrm{m}}\right)^2 + \frac{1}{R_\mathrm{ac}^2}\right)\left(-\omega L_\mathrm{r} - \frac{-\omega C_\mathrm{par} + \dfrac{1}{\omega L_\mathrm{m}}}{\left(\omega C_\mathrm{par} - \dfrac{1}{\omega L_\mathrm{m}}\right)^2 + \dfrac{1}{R_\mathrm{ac}^2}} + \frac{1}{\omega C_\mathrm{r}}\right)\right] \tag{5}$$

and

$$|i_\mathrm{r}(t)| = \frac{\hat{V}_\mathrm{1,sw}}{\sqrt{\left(\omega L_\mathrm{r} + \dfrac{-\omega C_\mathrm{par} + \dfrac{1}{\omega L_\mathrm{m}}}{\left(\omega C_\mathrm{par} - \dfrac{1}{\omega L_\mathrm{m}}\right)^2 + \dfrac{1}{R_\mathrm{ac}^2}} - \frac{1}{\omega C_\mathrm{r}}\right)^2 + \dfrac{1}{R_\mathrm{ac}^2\left(\left(\omega C_\mathrm{par} - \dfrac{1}{\omega L_\mathrm{m}}\right)^2 + \dfrac{1}{R_\mathrm{ac}^2}\right)^2}}}. \tag{6}$$

The influence of the parasitic capacitances and of the load on the resonant current can be seen in Fig. 4 (a) and (b) respectively. With this, the ZVS behavior can be explained as followed. A system with higher C_par results in a lower amplitude and a smaller phase shift. A rise of the output load increases the amplitude but lowers the phase shift. These two modifications lower Q_res down to a value where Q_res is not sufficient to fully load $\mathrm{C_{oss,t}}$. This leads to incomplete ZVS.

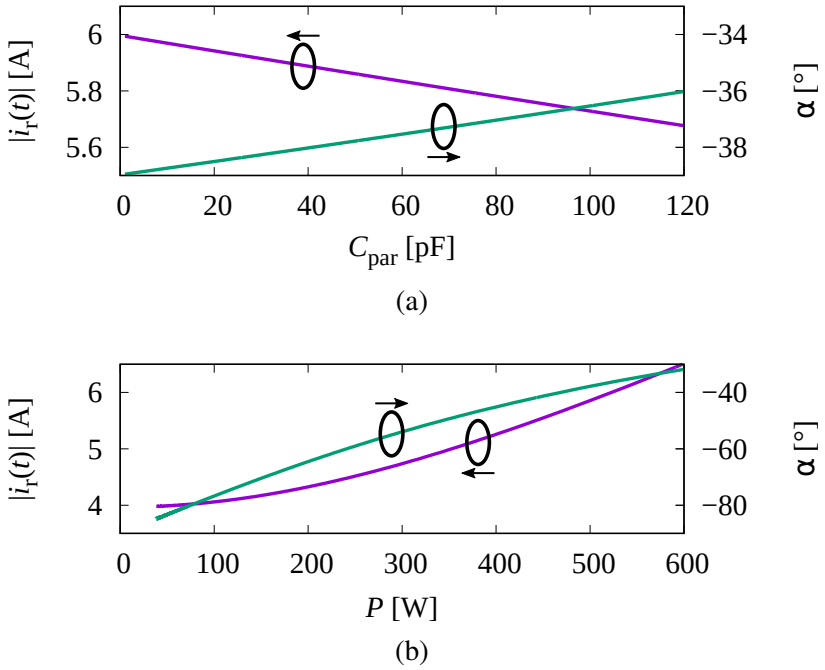

Fig. 4: Influence of (a) the parasitic capacitance C_{par} (P = 500 W) and of (b) the load P (C_{par} = 50 pF) on the resonant current $i_r(t)$. The influence on the magnitude of $i_r(t)$ and on α, the phase shift between $i_r(t)$ and $v_{1,sw}(t)$ is shown.

Experimental Results

The described ZVS behavior is confirmed by measurement results, see Fig. 5. While transmitting 300 W, ZVS is achieved with both dead-times of 45 ns and 65 ns. The system works more efficiently with a dead-time of 45 ns due to the longer lossy reverse conduction mode that comes with a dead-time of 65 ns. (Since the GaN HEMTs are driven with on- and off-state gate voltages of 6 V and −4 V to prevent parasitic turn-on, there is a large reverse conduction voltage of approx. 7 V, which is why the reverse conduction mode should be as brief as possible.) While transferring 500 W, the system is more efficient with a dead-time of 65 ns because a dead-time of 45 ns is too short to fully charge $C_{oss,t}$, which leads to incomplete ZVS.

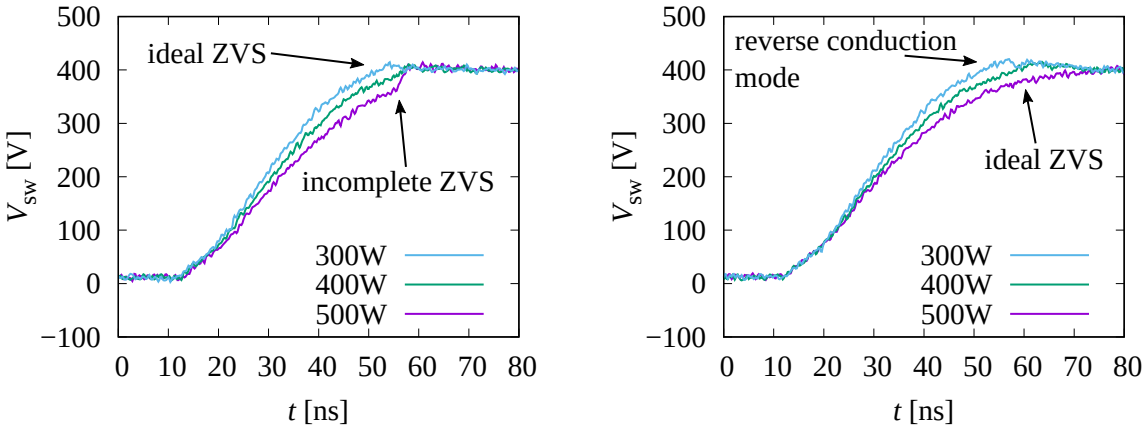

Fig. 5: Measurement results of a switch-on event with different output power and dead-time t_d of (a) 45 ns and (b) 65 ns

In systems similar to the presented one, where the values of L_m and L_r are in the same range, C_par influences the ZVS behavior more than in conventional LLC converters due their comparatively smaller magnetizing current caused by higher values of L_m. Because of this, rectifying diodes with a low junction capacitance and a transformer design with a low parasitic capacitance are mandatory.

Adaptive Dead-Time Control

As described before, the ZVS behavior of the system is load-dependent, which asks for a dead-time control to achieve higher efficiency. In the presented WPT system the switching frequency is set to a fixed value of 2 MHz. The receiving side is passive and does not communicate with the transmitting side, meaning that the output load is unknown to the transmitting side. Therefore, an adaptive control is realized in which the input current is measured and the dead-time is set accordingly. In Fig. 6, the experimental setup is shown schematically.

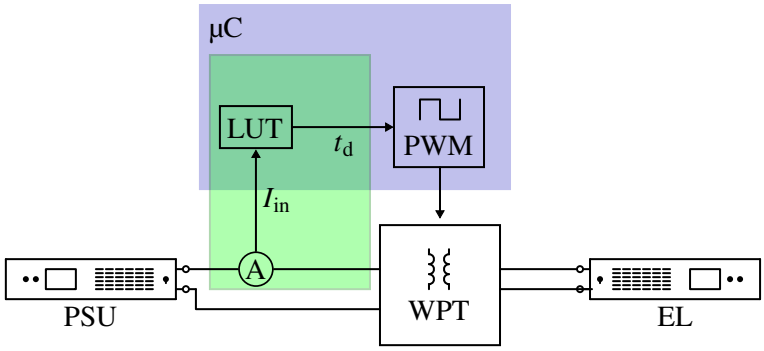

Fig. 6: Schematic of the experimental setup. The WPT system is placed between the power supply unit (PSU) and the electronic load (EL). The efficiency is measured with a precision power analyzer (not shown). The green area marks the dead-time adaption. There, the input current is measured with a hall sensor (A). Based on this value, the dead-time is adapted with a look-up table (LUT).

The input current is measured with a hall sensor (TMCS1101) which is directly connected to the µC. There, a predetermined dead-time is selected with a look-up table (LUT) based on the measured input current I_in. To set the dead-time accurately, a µC (STM32F334R8T6) with high-resolution PWM (HRPWM) is used, allowing to adjust the dead-time during operation with an accuracy of 217 ps. To fill the LUT, the input-current-dependent efficiency is measured for different dead-times as shown in Fig. 7. As described before, the optimal switching moment is when the charging of $C_\mathrm{oss,t}$ is just completed.

The peak efficiency of 92.9 % at $I_\mathrm{in} = 1.32$ A is achieved with a dead-time of 65 ns. Between an input current of 0.99 A and 1.28 A, a dead-time of 55 ns is more efficient. Below 0.99 A, the efficiency can be increased with $t_\mathrm{d} = 45$ ns. The enveloping curve in Fig. 7 shows that a finer resolution of the LUT is not needed. Furthermore, it can be seen that there is no further rise of the efficiency with a dead-time of 75 ns due to incomplete ZVS at higher values of I_in and a longer duration of the dead-time than the zero crossing of $i_\mathrm{r}(t)$. Thus, $C_\mathrm{oss,t}$ is slightly discharged again before the switching moment.

With the determined boundaries, an adaptive control of the dead-time can be realized. The system efficiency with dead-time control (green line) and with a fixed dead-time of 65 ns (dashed purple line) is shown in Fig. 8. With the dead-time control, the average efficiency can be raised. For example, the efficiency can be raised from 90.6 % to 91.1 % and from 91.6 % to 92 % while transferring 250 W and 300 W respectively, see Fig. 8.

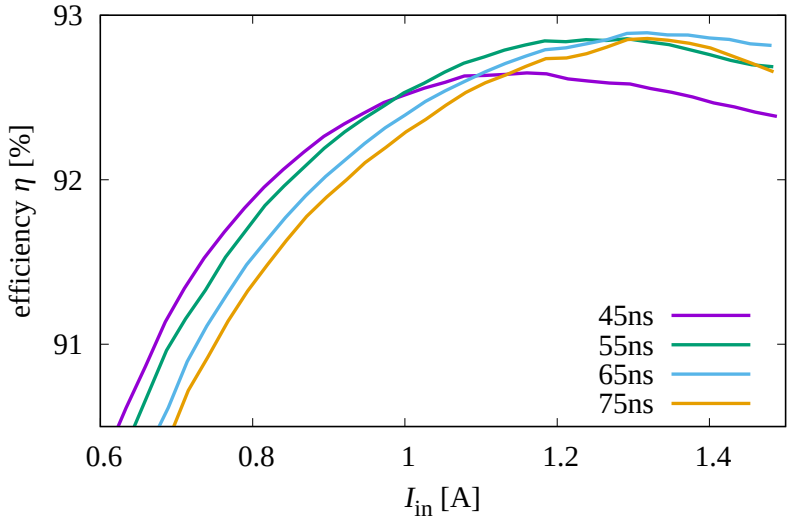

Fig. 7: Efficiency of the system with different dead-times depending on I_{in}.

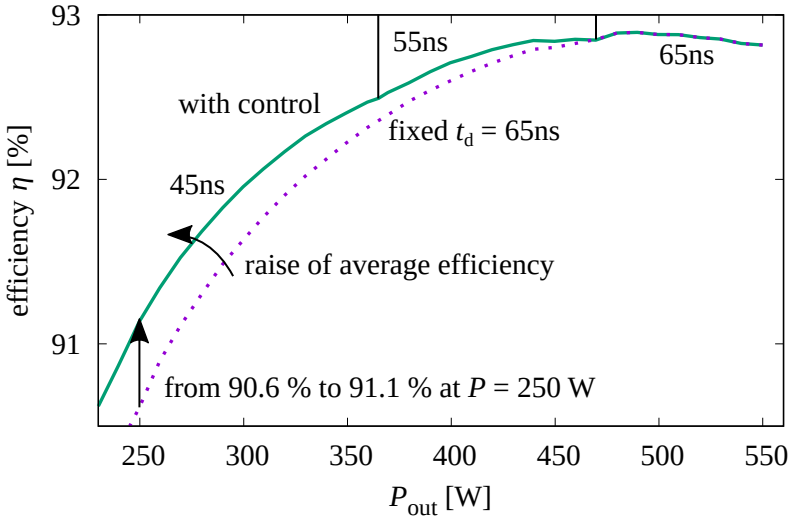

Fig. 8: System efficiency with and without adaptive dead-time control

Conclusion

This paper presents a detailed analysis of the ZVS behavior of a resonant inductive WPT system operating in the MHz range based on the LLC topology. The recharging process of the output capacitance of the half bridge and how it is influenced by parasitic capacitances and by load changes is investigated. Based on this, an adaptive dead-time control is realized by tuning the dead-time depending on the input current. This improves the efficiency over a wide range. This dead-time control is easily implemented and attractive for inductive resonant WPT systems where the receiving side does not communicate with the transmitting side.

References

[1] L. Gu, G. Zulauf, A. Stein, P. A. Kyaw, T. Chen, and J. M. R. Davila, "6.78-MHz wireless power transfer with self-resonant coils at 95% DCDC efficiency," *IEEE Transactions on Power Electronics*, vol. 36, no. 3, pp. 2456–2460, Mar. 2021.

[2] T. Krigar and M. Pfost, "2-MHz compact wireless power transfer system with voltage conversion from 400 V to 48 V," in *2021 IEEE Wireless Power Transfer Conference (WPTC)*, 2021.

[3] H. Wen, J. Gong, C.-S. Yeh, Y. Han, and J. Lai, "An investigation on fully zero-voltage-switching condition for high-frequency GaN based LLC converter in solid-state-transformer application," in *2019 IEEE Applied Power Electronics Conference and Exposition (APEC)*, 2019, pp. 797–801.

[4] H. Wen, Y. Liu, and J.-s. Lai, "Analysis on the effect of secondary side devices for the operation of GaN based LLC resonant converter," in *2020 IEEE Applied Power Electronics Conference and Exposition (APEC)*, 2020, pp. 2214–2218.

[5] H. Chen and X. Wu, "Analysis on the influence of the secondary parasitic capacitance to ZVS transient in LLC resonant converter," in *2014 IEEE Energy Conversion Congress and Exposition (ECCE)*, 2014, pp. 4755–4760.

[6] W. Qin, L. Zhang, and X. Wu, "Re-examination of ZVS condition for MHz LLC converter operating at resonant frequency," in *2018 IEEE International Power Electronics and Application Conference and Exposition (PEAC)*, 2018, pp. 1–4.

[7] C. Oeder and T. Duerbaum, "ZVS investigation of LLC converters based on FHA assumptions," in *2013 Twenty-Eighth Annual IEEE Applied Power Electronics Conference and Exposition (APEC)*, 2013, pp. 2643–2648.